

Rovibrational effects on nuclear shielding of apex nuclei in bent molecules

H.-Jörg Osten

Academy of Sciences of the GDR, Central Institute of Physical Chemistry, 1199 Berlin, Rudower Chaussee 6, German Democratic Republic

Cynthia J. Jameson

Department of Chemistry, University of Illinois at Chicago, Chicago, Illinois 60680

(Received 30 November 1984; accepted 5 February 1985)

The isotope shifts of non-end nuclei with lone pairs are generally larger than those of nuclei without lone pairs. Using the bent triatomic molecule as a prototype, we examine the mass and temperature dependence of the mean bond angle deformation and the mean displacement along a bond due to centrifugal stretching and anharmonic vibration. We find that the temperature dependence of $\langle \Delta \alpha \rangle$ determines whether the temperature dependence of the shielding of the apex nucleus will be normal [$(d\sigma_0/dT) < 0$] or abnormal. The dominant contribution of the rotation to the temperature dependence of $\langle \Delta \alpha \rangle$ in the hydrides can lead to opposing temperature effects on shielding while the mass effects lead to normal isotope shifts. We performed similar calculations for the trigonal pyramidal molecules in order to explain the observed abnormal temperature dependence of the ^{15}N and ^{31}P nuclear shielding in NH_3 and PH_3 .

I. INTRODUCTION

The effects of intermolecular interactions and intramolecular dynamics on the shielding of nuclei in semirigid molecules can be expressed empirically as a function of temperature T and of gas density ρ :

$$\sigma(T, \rho) = \sigma_0(T) + \sigma_1(T)\rho + \sigma_2(T)\rho^2 + \dots, \quad (1)$$

in which the parameters which are empirical functions of temperature are interpreted as follows:

$$\sigma_0(T) = \sigma_e + \sum_i (\partial\sigma/\partial q_i)_e \langle q_i \rangle^T + \dots \quad (2)$$

$$= \sigma_e + \sum_i (\partial\sigma/\partial \Delta r_i)_e \langle \Delta r_i \rangle^T + \sum_{ij} (\partial\sigma/\partial \Delta \alpha_{ij})_e \langle \Delta \alpha_{ij} \rangle^T + \dots, \quad (3)$$

$$\sigma_1(T) = \int_{\Omega} \int_R [\sigma(R, \Omega) - \sigma(\infty)] \times \exp[-V(R, \Omega)/kT] dR d\Omega. \quad (4)$$

$\sigma_0(T)$ is the shielding of a single molecule averaged with respect to changes in bond distances r and bond angles α . $\sigma_1(T)$ is the change in shielding with intermolecular distances R and orientations Ω , averaged over the intermolecular potential. In this paper we will not consider intermolecular effects.

The isotope shifts observed in NMR are due to differences in the $\langle \Delta r_i \rangle^T$ and $\langle \Delta \alpha_{ij} \rangle^T$ in Eq. (3) for isotopically related molecules. There has been increasing interest in NMR isotope shifts,¹ a dynamical property, as well as in the derivatives of nuclear shielding, $(\partial\sigma/\partial \Delta r_i)_e$, $(\partial\sigma/\partial \Delta \alpha_{ij})_e$, etc., which are purely electronic properties.^{2,3}

In previous papers we have considered the temperature dependence and isotope shifts due to rovibrational averaging of nuclear shielding of end atoms such as ^{19}F .^{4,5} We have shown how it is possible to interpret the observed temperature dependence of ^{19}F nuclear shielding $\sigma_0(T)$ in terms of shielding derivatives $(\partial\sigma/\partial \Delta r)_e$, with which it is also possible to reproduce observed isotope shifts.⁵ We have examined

the isotope shifts of centrally located atoms without lone pairs (e.g., ^{13}C in CH_4) and we have shown that the shielding derivatives can be obtained directly from observed isotope shifts in these cases.⁶

The effects of rovibrational averaging on the shielding of a nucleus in a molecular structure involving nonvanishing mean bond angle displacements about the nucleus (such as N in NH_3 or NO_2^-) are demonstrably different from that of a nucleus in a more symmetrical bond arrangement (such as N in NH_4^+). The origin of the differences is not easily established since the less symmetrical arrangements which allow for a nonvanishing mean bond angle deformation (such as Se in H_2Se , N in NH_3 , or P in PH_3) also involve lone pairs on the observed nucleus. The dynamic factors are qualitatively different: For a symmetrical environment such as ^{13}C in CH_4 , $\langle \Delta \alpha_{ij} \rangle^T$ terms are usually neglected, since the sum of the mean bond angle changes nearly vanishes. The contribution to the temperature dependence in the zero-pressure limit $\sigma_0(T)$, and to the isotope shift of ^{13}C in such environments are then largely due to the leading $\langle \Delta r \rangle^T$ terms. In the less symmetrical site typified by ^{15}N in NH_3 , nonvanishing angle deformation terms contribute to the vibrationally averaged shielding so that the temperature dependence of the N shielding in the zero-pressure limit and the ^{15}N isotope shift involve $\langle \Delta \alpha \rangle^T$ as well as $\langle \Delta r \rangle^T$ terms.

In addition to the geometrical and dynamic factors, there may be important differences between the highly symmetrical and the less symmetrical nuclear sites in their shielding sensitivity to bond extension. Since the less symmetric geometrical arrangement is usually a consequence of the presence of lone pairs on the observed nucleus, the nature of the electronic factors are undoubtedly quantitatively, if not qualitatively different.

II. ISOTOPE SHIFTS FOR NON-END NUCLEI WITH LONE PAIRS

In Table I we demonstrate the generally larger isotope shifts observed for nuclei in sites involving nonvanishing

TABLE I. Isotope shifts $^1\Delta = \sigma^A(A^mX\ldots) - \sigma^A(A^{m'}X\ldots)$ in ppm per substitution, for molecules with nonvanishing mean bond angle deformations. Reduced isotope shifts [Eq. (5)] for these systems compared with analogous nuclear sites of higher symmetry.

Obs. nucleus	Molecule	m'/m	$-^1\Delta/\text{ppm}$	$-2^1\Delta/\text{ppm}$ $m_A(m' - m)/m'(m_A + m)$	
^{15}N	NH_3	$2/^{1}\text{H}$	0.65 ^a	2.8	1.32 in NH_4^{+k}
	NO_2^-	$18/^{16}\text{O}$	0.138 ^{b,c}	5.14	2.1 in NO_3^{-c}
^{31}P	$>\text{P}-\text{H}$		up to 1.30 ^d	up to 5.2	
	PH_3	$2/^{1}\text{H}$	0.843 ^e	3.48	
	PCl_3	$37/^{35}\text{Cl}$	0.019 ^f	1.5	0.52 in PO_4^{4-}
	PBr_3	$81/^{79}\text{Br}$	0.006 ^f	1.7	
^{17}O	H_2O	$2/^{1}\text{H}$	1.54 ^g	6.54	
^{77}Se	H_2Se	$2/^{1}\text{H}$	7.02 ^h	28.4	
	$\text{Se}-\text{C}$	$^{13}/^{12}\text{C}$	0.170–0.341 ⁱ	5.1–10.2 ^m	0.67 in RSeCl_3
	R_1Se	$^{82}/^{74}\text{Se}$	0.0786, 0.103	3.16, 4.14 ^m	
	R_2Se		0.11, 0.139 ^j	4.43, 5.57 ^m	
^{125}Te	$\text{Te}-\text{C}$	$^{13}/^{12}\text{C}$	0.32–0.34 ⁱ	9.1–9.7 ^m	

^a Reference 39.

^b R. L. Van Etten and J. M. Risley, *J. Am. Chem. Soc.* **103**, 5633 (1981).

^c K. K. Andersson, S. B. Philson, and A. B. Hooper, *Proc. Natl. Acad. Sci. U.S.A.* **79**, 5871 (1982).

^d A. A. Borisenko, N. M. Sergeyev, and Yu. A. Ustynyuk, *Mol. Phys.* **22**, 715 (1971).

^e A. K. Jameson and C. J. Jameson, *J. Magn. Reson.* **32**, 455 (1978).

^f M. J. Buckingham, G. E. Hawkes, I. M. Ismail, and P. J. Sadler, *J. Chem. Soc. Dalton Trans.* **1982**, 1167.

^g O. Lutz and H. Oehler, *Z. Naturforsch. Teil A* **32**, 131 (1977).

^h Reference 31.

ⁱ Reference 7.

^j Reference 8.

^k R. E. Wasylshen and J. O. Friedrich, *J. Chem. Phys.* **80**, 585 (1984).

^l O. Lutz, A. Nolle, and D. Staschewski, *Z. Naturforsch. Teil A* **33**, 380 (1978).

^m These are not directly comparable with above numbers, since substitution at other than an end atom has a mass effect on $\langle\Delta r\rangle$ which is not strictly given by the factor $\frac{1}{2}[(m' - m)/m'] \cdot [m_A/(m_A + m)]$.

mean bond angle deformations. These nuclei are characterized by an electronic distribution (the presence of lone pairs) which dictates the molecular geometry. The isotope shift for a nucleus in a symmetrical site, tetrahedral, e.g., is much smaller than that in a bent or pyramidal configuration, as for NH_4^+ compared to NH_3 . In the nearly tetrahedral RSeCl_3 , the $^{13}/^{12}\text{C}$ -induced Se isotope shift is -0.12 ppm compared to -0.17 up to -0.341 ppm for the bent configuration R_2Se .^{7,8}

We introduced the reduced isotope shift as a convenient nearly mass-independent quantity so as to compare magnitudes of isotope shifts for nuclei with different substituted atoms.⁹ The one-bond reduced isotope shift for nucleus A in isotopomers of $\text{AX}\ldots$ is

$$^1\Delta^R \equiv ^1\Delta \left[\frac{m' - m}{m'} \cdot \frac{1}{2} \frac{m_A}{(m_A + m)} \right]^{-1}, \quad (5)$$

where

$$^1\Delta = \sigma^A(A^mX\ldots) - \sigma^A(A^{m'}X\ldots),$$

where m_A is the mass of the observed nucleus, m' and m are the masses of the isotopes of X.

Although $^1\Delta^R$ is a meaningful quantity in the symmetrical case, in which it can be identified with $-(\partial\sigma/\partial\Delta r)_e \langle\Delta r_{AX}\rangle$ for symmetrical AX_n molecular types, it is not so obviously interpreted in the cases shown in Table I. There are two reasons for this. One is that the mass dependence of $\langle\Delta\alpha\rangle$ is not the same as that of $\langle\Delta r\rangle$ upon substitution of an end atom. Secondly, the mass dependence used in defining the reduced isotope shift is strictly the vibra-

tional contribution only, since the rotational motion does not contribute significantly to the isotope shift of nucleus A in the symmetrical AX_n molecular type. The rotational contribution to $\langle\Delta\alpha\rangle$ is not negligible for the bent AX_2 and the pyramidal AX_3 molecular types. Nevertheless, we will show in this paper that the contribution to the isotope shift by the angle deformation term is generally much smaller than that from the bond extension terms, so that it is still useful to calculate reduced isotope shifts as we have done previously. Table I shows that without exception, the nucleus in a less symmetrical case which involves lone pairs and nonvanishing mean bond angle deformations around the observed nucleus has a larger reduced isotope shift than the nucleus in the symmetrical AX_n case. Thus, we compare $\text{NH}_3/\text{NH}_4^+$ in which 2.8/1.32 are the reduced isotope shifts. Likewise we compare $\text{NO}_2^-/\text{NO}_3^- = 5.14/2.1$, $\text{PH}_3/\text{PO}_4^{4-} = (1.5 \text{ to } 5.2)/0.52$, and $\text{H}_2\text{Se}, \text{SeR}_1\text{R}_2, \text{R}_1\text{SeSeR}_2/\text{RSeCl}_3 = (3.1 \text{ to } 28.4)/0.67$. The general trend for larger isotope shifts when lone pair(s) constitute one or more of the localized electron pairs around the observed nucleus indicates that something is intrinsically different for the nuclei in these environments. We therefore pose the question of the possible reason for this. Is it a larger $(\partial\sigma/\partial\Delta r)_e$ associated with nucleus A having a lone pair or is it that a nonnegligible $\langle\Delta\alpha\rangle^T$ gives an additional contribution which is of the same (or opposite) sign as that from the bond extension term? The other intriguing observations which pose the same questions are the abnormal signs of $(d\sigma/dT)$ found for ^{15}N and ^{31}P in NH_3 and PH_3 .^{10,11} The normal temperature dependence

$(d\sigma_0/dT) < 0$ has been observed in all other nuclei, including the ^{31}P nucleus in one pyramidal environment PF_3 .¹²

In this paper we consider the dynamic factors which lead to nonvanishing angle deformation contributions to the vibrational averaging of shielding. Using the bent triatomic molecule as a prototypical system, we examine the mass and temperature dependence of $\langle \Delta\alpha \rangle$, and consider the implications of these with respect to normal vs abnormal $(d\sigma_0/dT)$ and isotope shifts. Since abnormal $(d\sigma_0/dT)$ have been observed for N and P in NH_3 and PH_3 , we also consider selected pyramidal molecules, examine the mass and the temperature dependence of $\langle \Delta\alpha \rangle$, and consider the factors which determine the sign of $(d\sigma_0/dT)$ for the apex nucleus in a pyramidal molecule.

III. THE BENT TRIATOMIC MOLECULE

The general temperature and mass dependence of the thermal average bond length is well established theoretically and experimentally. Experimentally, electron diffraction data show the thermal average bond length $\langle r \rangle = r_g$ increasing with temperature, and microwave spectroscopy shows that $\langle r^{-2} \rangle^{-1/2} = r_0 > r_e$. This is completely consistent with an average over an anharmonic bond stretching potential, such as the Morse potential, and a centrifugal stretching which tends to lengthen bonds as the molecule rotates. The mass dependence of the thermal average bond length is also well established, the average deviation from r_e is larger when lighter atoms are involved. On the other hand, the thermal average bond angle is not so well characterized. In electron diffraction, average distances between nonbonded atoms are also observed and from this an average bond angle can be inferred but not so unequivocally because the increase in the distance between nonbonded atoms with increasing temperature in a bent triatomic such as SO_2 is partly due to the increase in the S–O mean bond distance and only partly due to the change in the mean bond angle. From microwave spectroscopy an average bond angle can be inferred from the moments of inertia, again not so unequivocally. The anharmonicity of angle bending potentials are less well known, there is no successful model which is the counterpart of the Morse potential. The effects of centrifugal distortion on the bond angle are not so well established. In fact, both $\langle \alpha \rangle^T > \alpha_e$ and $\langle \alpha \rangle^T < \alpha_e$ have been quoted for NH_3 , e.g., and it is not firmly established which of $\langle \text{HXH} \rangle^T$ or $\langle \text{DXD} \rangle^T$ is larger in XH_2 - or XH_3 -type molecules. The answers to these questions determine the effects of bond angle deformation on the observed isotope shifts and temperature dependence of σ_0 . In this paper we attempt to answer these questions by computations using molecules with nonvanishing average bond angle deformations and for which good anharmonic force fields are available.

In the investigation of the effects of bond angle deformation on the average nuclear magnetic shielding, the logical simplest system to study is the bent triatomic molecular type. In this case there are six cubic force constants which are explicitly related to vibration-rotation interaction constants which can be obtained from the microwave spectrum.¹³ The cubic part of the anharmonic force field has been determined in this way for O_3 , OF_2 , SO_2 , SeO_2 , H_2O ,

H_2S , and H_2Se . For these molecules quartic potentials are available from a combination of rotational and vibrational analyses. We use six bent triatomics as illustrative examples: H_2O , H_2S , H_2Se , O_3 , SO_2 , and SeO_2 . H_2O is a logical choice, since it is the lightest stable bent triatomic; *ab initio* calculations have also provided anharmonic force constants. For example, Krohn, Ermler, and Kern calculated vibrational state averages for $\langle \Delta r \rangle$, $\langle \Delta \alpha \rangle$ and electronic properties for the H_2O molecule based on *ab initio* potential surfaces.¹⁴ Shavitt's *ab initio* force field¹⁵ has been found in agreement with the experimental force field of Hoy, Mills, and Streyl¹⁶ by the method of comparison of molecular potential energy surfaces devised by Lacy and Whiffen.¹⁷ In addition, there is an *ab initio* theoretical nuclear shielding surface for H_2O by Fowler, Riley, and Raynes,³ over which vibrational state averages have been carried out.¹⁸ O_3 is of interest because there are calculations of the ^{17}O shielding of both types of oxygen nuclei in O_3 for several bond lengths and bond angles.¹⁹ H_2Se is an interesting molecule from the point of view that the isotope shift is one of the largest ever observed, 7 ppm per D substitution. There is also a fairly recent force field for H_2Se by Skotnikov and Sverdlov.²⁰ SO_2 is of interest for different reasons. The temperature dependent structure of SO_2 which has been measured by electron diffraction by Mawhorter and Finks provides empirical values of mean bond lengths.²¹ Kohl and Hilderbrandt's variational wave function analysis relates the vibrationally averaged distances measured by electron diffraction to r_e , and from their results we obtain the mean bond displacements $\langle \Delta r \rangle^T$ by difference.²² Whitehead and Handy²³ have shown that the vibrational frequencies calculated variationally from a potential with the Kuchitsu and Morino force constants²⁴ (which we use here) give agreement with experiment to $\pm 1 \text{ cm}^{-1}$ for the fundamentals of SO_2 . Carter and Muller have developed a method for obtaining analytic potential energy functions of triatomic molecules from a combination of spectroscopy, *ab initio* calculations and thermodynamic data directly.²⁵ They find that their analytic potential function for SO_2 , the quadratic and the larger cubic and quartic force constants calculated by differentiating the surface at the equilibrium configuration, are in agreement with the experimental anharmonic force field for this molecule. SeO_2 completes the logical sequence, OH_2 , SH_2 , SeH_2 , O_3 , SO_2 , SeO_2 , so that we may compare trends which relate to the size of the apex atom.

A. Dynamic calculations

The bent triatomic dynamic calculations were carried out using a potential of the form

$$\begin{aligned} V = & \frac{1}{2} f_r [(\Delta r_1)^2 + (\Delta r_2)^2] + \frac{1}{2} f_\alpha (r \Delta \alpha)^2 + f_{rr} (\Delta r_1) (\Delta r_2) \\ & + f_{r\alpha} [(\Delta r_1) (r \Delta \alpha) + (\Delta r_2) (r \Delta \alpha)] \\ & + f_{rrr} [(\Delta r_1)^3 + (\Delta r_2)^3] \\ & + f_{rrr} [(\Delta r_1) + (\Delta r_2)] (\Delta r_1) (\Delta r_2) \\ & + f_{r\alpha\alpha} [(\Delta r_1)^2 + (\Delta r_2)^2] (r \Delta \alpha) + f_{rr\alpha} (\Delta r_1) (\Delta r_2) (r \Delta \alpha) \\ & + f_{r\alpha\alpha} [(\Delta r_1) + (\Delta r_2)] (r \Delta \alpha)^2 + f_{\alpha\alpha\alpha} (r \Delta \alpha)^3. \end{aligned} \quad (6)$$

The mean displacements $\langle \Delta r \rangle$ and the mean angle deforma-

tions $\langle \Delta\alpha \rangle$ are obtained from the solutions of the following linear coupled equations, according to the method of Bartell,²⁶ described in detail previously.²⁷

$$(f_r + f_{rr})\langle \Delta r \rangle + f_{r\alpha}\langle r\Delta\alpha \rangle = -(3f_{rrr} + f_{rrr'})\langle (\Delta r)^2 \rangle - \left(f_{r\alpha\alpha} - \frac{1}{2r}f_{r\alpha}\right)\langle (r\Delta\alpha)^2 \rangle - 2f_{rrr'}\langle \Delta r_1\Delta r_2 \rangle - \left(2f_{rr\alpha} + f_{rr'\alpha} - \frac{1}{r}f_{r\alpha}\right)\langle (\Delta r)(r\Delta\alpha) \rangle, \quad (7)$$

$$2f_{r\alpha}\langle \Delta r \rangle + f_{\alpha}\langle (\Delta\alpha)^2 \rangle = -2f_{rr\alpha}\langle (\Delta r)^2 \rangle - \left(3f_{\alpha\alpha\alpha} + \frac{1}{2r}f_{r\alpha}\right)\langle (r\Delta\alpha)^2 \rangle - f_{rr'\alpha}\langle (\Delta r_1)(\Delta r_2) \rangle - \left(4f_{r\alpha\alpha} + \frac{1}{2r}(f_r + f_{rr})\right)\langle (\Delta r)(r\Delta\alpha) \rangle. \quad (8)$$

The mean square amplitudes $\langle \Delta r_i^2 \rangle$, $\langle \Delta r_i\Delta r_j \rangle$, etc. are calculated in the usual manner in terms of $\langle Q_i^2 \rangle = (\hbar/4\pi^2c\omega_i) \coth(\hbar c\omega_i/2kT)$. The centrifugal stretching due to rotation is linear with temperature and is given in closed form by Toyama, Oka, and Morino.²⁸ These allow us to obtain $\langle \Delta r \rangle$ and $\langle \Delta\alpha \rangle$ using the molecular constants given in Table II. Some typical results are shown in Table III.

The rotational contribution to the temperature dependence of $\langle \Delta r \rangle$ and $r\langle \Delta\alpha \rangle$ of H₂O agrees with that of Toyama *et al.*²⁸ who obtained $\langle \Delta r_{OH} \rangle_{\text{rot}} = 2.75 \times 10^{-6}$ Å and $r\langle \Delta\alpha \rangle_{\text{rot}} = -6.0 \times 10^{-6}$ T compared with our 2.92×10^{-6} and -7.16×10^{-6} T. For D₂O their values are 2.74×10^{-6} and -5.52×10^{-6} T compared to our 2.90×10^{-6} and -6.7×10^{-6} T, all in Å. Our mean bond displacements can also be compared with various calculations by Bartell²⁶: $\langle \Delta r_{OH} \rangle_{\text{vib}} = 0.0182, 0.0171, \text{ and } 0.0173$ Å, $\langle \Delta r_{OD} \rangle_{\text{vib}} = 0.0131, 0.0125$ Å, $r\langle \Delta\alpha \rangle_{\text{vib}} = 5.0 \times 10^{-4}, 2.2 \times 10^{-3}$ Å for H₂O and $1.6 \times 10^{-4}, 1.3 \times 10^{-3}$ for D₂O, by various methods. Our values are $\langle \Delta r_{OH} \rangle_{\text{vib}} = 0.0191$, $\langle \Delta r_{OD} \rangle_{\text{vib}} = 0.0139$ Å, $r\langle \Delta\alpha \rangle_{\text{vib}} = 2.17 \times 10^{-3}$ and 2.0×10^{-3} Å for H₂O and D₂O, respectively. All these averages are calculated for 0 K. Our results for H₂O are in agreement with Krohn, Ermler, and Kern,¹⁴ and with Fowler and Raynes¹⁸ who also obtain $\langle \Delta\alpha \rangle_{\text{vib}} > 0$, and with Kohl and Hilder-

brandt's averages²²: $\langle \Delta r_{OH} \rangle_{\text{vib}} = 0.017$ Å, $\langle \Delta r_{OD} \rangle_{\text{vib}} = 0.0125$ Å at 300 K.

We compare our results for SO₂ with those of Ma-whorter and Fink²¹ who measured $r_g(\text{S-O})$ and $r_g(\text{O-O})$ as a function of temperature with electron diffraction techniques. Both increase with increasing temperature, that is $[\langle \Delta r_{SO} \rangle^{400} - \langle \Delta r_{SO} \rangle^{200}] > 0$. The precision of their data does not permit the unequivocal determination of the sign of $r[\langle \Delta\alpha_{OSO} \rangle^{400} - \langle \Delta\alpha_{OSO} \rangle^{200}]$. However, their results are not inconsistent with the negligible change of bond angle with increasing temperature shown in Table III. They calculate the rotational contribution to the temperature dependence of $\langle \Delta r_{SO} \rangle$ as 1.5×10^{-6} Å/deg, compared to our 1.52×10^{-6} Å/deg in Table III. Kohl and Hilderbrandt²² have calculated $\langle \Delta r_{SO} \rangle_{\text{vib}}$ as a function of temperature by a variational calculation using a product basis set of anharmonic oscillator wave functions based on Kuchitsu and Morino's²⁴ force constants. At 300 K they obtain 0.004 74 Å where we have 0.0047. Between 300 and 600 K they obtain a change in $\langle \Delta r_{SO} \rangle$ of 2.7×10^{-6} Å/deg, while we get a change of 2.2×10^{-6} Å/deg. We have used a more recently available force field. We note that for SO₂, our use of harmonic oscillator partition functions in evaluating $\langle Q_i^2 \rangle^T$ gives results indistinguishable from those of Kohl and Hilderbrandt at 300 K. The $\coth(\hbar c\omega_i/2kT)$ function is a closed form which results from the complete sum of a geometric series when harmonic vibrational levels are used. On the other hand, the sum over the anharmonic levels is a truncated sum involving somewhat lower energies. Fowler and Raynes¹⁸ have shown that for H₂O, the use of the latter gives mean bond displacements which are somewhat shorter than those obtained using $\coth(\hbar c\omega_i/2kT)$. Certainly for molecules with many more than two or three vibrational modes, truncation of the sum becomes a problem. The coth terms on the other hand, are few and very simple to calculate.

B. General trends

The results shown in Table III can be summarized as follows: As is generally found for other molecules, vibration-

TABLE II. Potential parameters used in dynamic calculations for bent triatomics.

	H ₂ O ^a	H ₂ S ^b	H ₂ Se ^c	O ₃ ^d	SO ₂ ^b	SeO ₂ ^e
$r_e/\text{Å}$	0.9572	1.336	1.4605	1.2717	1.4308	1.6070
α_e/deg	104.5	92.2	90.8	116.8	119.3	113.8
$f_r/\text{mdyn Å}^{-1}$	8.4588	4.284	3.5114	6.163	10.332	6.91
f_α	0.7834	0.429	0.3345	1.3	0.815	0.488
f_{rr}	-0.0948	-0.012	-0.0248	1.602	0.081	0.030
$f_{r\alpha}$	0.3920	0.101	0.0946	0.402	0.227	0.009
$f_{rrr}/\text{mdyn Å}^{-2}$	-10.1664	-3.862	-2.9989	-9.15	-11.846	-11.50
$f_{rrr'}$	-0.4044	+0.022	+0.0179	-1.32	-0.457	-0.15
$f_{rr\alpha}$	-0.3979	-0.299	-0.1015	-1.24	-0.475	+0.093
$f_{rr'\alpha}$	-0.5736	-0.112	-0.0241	-1.02	-0.531	-0.062
$f_{r\alpha\alpha}$	-0.4891	-0.030	-0.0257	-1.22	-0.440	-0.155
$f_{\alpha\alpha\alpha}$	-0.2325	-0.008	-0.0197	-0.31	-0.139	-0.024

^a D. F. Smith and J. Overend, *Spectrochim. Acta Part A* **28**, 483 (1972).

^b Reference 24.

^c Reference 20.

^d A. Barbe, C. Secroun, and P. Jouve, *J. Mol. Spectrosc.* **49**, 171 (1974).

^e H. Takeo, E. Hirota, and Y. Morino, *J. Mol. Spectrosc.* **34**, 370 (1970).

TABLE III. Mean bond displacements and mean bond angle deformations at $T = 300$ K, isotope effects ($\Delta_{\text{iso}} \equiv \langle \Delta r \rangle_{\text{light}}^{300} - \langle \Delta r \rangle_{\text{heavy}}^{300}$, or $r\langle \Delta r \rangle_{\text{light}}^{300} - r\langle \Delta r \rangle_{\text{heavy}}^{300}$) and temperature dependence ($\Delta_T \equiv \langle \Delta r \rangle^{400} - \langle \Delta r \rangle^{200}$ or $r\langle \Delta \alpha \rangle^{400} - r\langle \Delta \alpha \rangle^{200}$) for bent triatomic molecules.

	$\langle \Delta r \rangle$			$r\langle \Delta \alpha \rangle$		
	Vib.	Rot.	Tot.	Vib.	Rot.	Tot.
$\text{H}_2\text{O}/10^{-2} \text{ \AA}$	1.915	0.088	2.003	0.218	-0.215	0.003
$\text{D}_2\text{O}/10^{-2} \text{ \AA}$	1.391	0.087	1.478	0.211	-0.201	0.010
$\Delta_{\text{iso}}/10^{-3} \text{ \AA}$	5.237	0.006	5.243	0.075	-0.141	-0.066
$\Delta_T/10^{-4} \text{ \AA}$	0.085	5.846	5.931	0.083	-14.340	-13.508
$\text{H}_2\text{S}/10^{-2} \text{ \AA}$	1.836	0.110	1.947	0.129	-0.067	0.062
$\text{D}_2\text{S}/10^{-2} \text{ \AA}$	1.318	0.110	1.428	0.126	-0.057	0.069
$\Delta_{\text{iso}}/10^{-3} \text{ \AA}$	5.181	0.002	5.181	0.034	-0.104	-0.070
$\Delta_T/10^{-4} \text{ \AA}$	0.309	7.364	7.673	0.249	-4.505	-4.256
$\text{H}_2\text{Se}/10^{-2} \text{ \AA}$	1.925	0.124	2.049	-0.183	-0.076	-0.260
$\text{D}_2\text{Se}/10^{-2} \text{ \AA}$	1.373	0.124	1.497	-0.101	-0.071	-0.172
$\Delta_{\text{iso}}/10^{-3} \text{ \AA}$	5.514	0.001	5.515	-0.826	-0.054	-0.880
$\Delta_T/10^{-4} \text{ \AA}$	0.553	8.272	8.825	2.286	-5.101	-2.815
$\text{O}_3/10^{-2} \text{ \AA}$	0.809	0.069	0.878	0.127	-0.122	0.004
$^{18}\text{O}_2\text{O}/10^{-2} \text{ \AA}$	0.787	0.069	0.856	0.122	-0.120	0.002
$\Delta_{\text{iso}}/10^{-3} \text{ \AA}$	0.224	0.001	0.225	0.050	-0.022	0.028
$\Delta_T/10^{-4} \text{ \AA}$	4.378	4.615	8.993	3.382	-8.126	-4.744
$\text{O}_2\text{S}/10^{-2} \text{ \AA}$	0.471	0.046	0.516	0.283	-0.179	0.104
$^{18}\text{O}_2\text{S}/10^{-2} \text{ \AA}$	0.454	0.046	0.500	0.282	-0.176	0.106
$\Delta_{\text{iso}}/10^{-3} \text{ \AA}$	0.171	0.001	0.172	0.015	-0.031	-0.016
$\Delta_T/10^{-4} \text{ \AA}$	2.138	3.041	5.179	7.385	-11.965	-4.579
$\text{O}_2\text{Se}/10^{-2} \text{ \AA}$	0.737	0.056	0.793	0.111	-0.193	-0.082
$^{18}\text{O}_2\text{Se}/10^{-2} \text{ \AA}$	0.707	0.056	0.763	0.113	-0.189	-0.076
$\Delta_{\text{iso}}/10^{-3} \text{ \AA}$	0.299	0	0.299	-0.017	-0.037	-0.054
$\Delta_T/10^{-4} \text{ \AA}$	6.525	3.730	10.256	4.469	-12.845	-8.376

al and rotational contributions to the mean bond displacements $\langle \Delta r \rangle$, are positive. As usual, the temperature dependence leads to $[\langle \Delta r \rangle^{400} - \langle \Delta r \rangle^{200}] > 0$, and for the XH bonds this is dominated by rotational contributions because the higher vibrational frequencies for these molecules lead to a smaller temperature dependence in the $(1/\omega)\coth(hc\omega/2kT)$ terms appearing in the vibrational average. The rotational contribution, on the other hand, is linear with temperature. The magnitude of the isotope effect on the bond length at 300 K, $[\langle \Delta r_{\text{XH}} \rangle - \langle \Delta r_{\text{XD}} \rangle]$ is dominated by vibration in all cases.

The vibrational contribution to the mean bond angle deformation $\langle \Delta \alpha \rangle_{\text{vib}}$ is of either sign, i.e., in some of the molecules studied here the average bond angle is greater than the equilibrium value, in others it is smaller. In all cases, however, $\langle \Delta \alpha \rangle_{\text{vib}}$ increases algebraically with increasing temperature so that $[\langle \Delta \alpha \rangle_{\text{vib}}^{400} - \langle \Delta \alpha \rangle_{\text{vib}}^{200}] > 0$ for all, with smaller changes with temperature for the hydrides due to the greater vibrational frequencies. The rotational contribution to the mean bond angle deformation $\langle \Delta \alpha \rangle_{\text{rot}}$ is negative for all bent triatomics and changes linearly with T so that $[\langle \Delta \alpha \rangle_{\text{rot}}^{400} - \langle \Delta \alpha \rangle_{\text{rot}}^{200}] < 0$. These findings can be understood in terms of the predominant centrifugal stretching effects arising from the rotation about the principal axis parallel to the line connecting the two end atoms. Vibration and rotation contributions add up to $[\langle \Delta \alpha \rangle^{400} - \langle \Delta \alpha \rangle^{200}] < 0$, more pronounced for the hydrides, in which the vibrational contribution is small. Thus, the temperature dependence of $\langle \Delta r \rangle$ and $r\langle \Delta \alpha \rangle$ are opposite in sign. The magnitudes of $[\langle \Delta r \rangle^{400} - \langle \Delta r \rangle^{200}]$ and $r[\langle \Delta \alpha \rangle^{400} - \langle \Delta \alpha \rangle^{200}]$ are comparable in the hydrides (0.5–2.0):1.0, whereas in the oxides the

temperature dependence of $\langle \Delta \alpha \rangle$ is negligible compared to that of $\langle \Delta r \rangle$, except for SeO_2 where the mass ratio of the end and central atom approaches that of a hydride, and the centrifugal stretching dominates $r\langle \Delta \alpha \rangle$ again.

It now becomes necessary to explain this dichotomy, i.e., to determine whether this result is a consequence of fundamental qualitative differences in the potential energy surface of the hydrides and the others or whether the different masses of the ligands (1 vs 16 amu) is responsible. To answer this question, we examined the mass dependence of $[\langle \Delta r \rangle^{400} - \langle \Delta r \rangle^{200}]$ and $r[\langle \Delta \alpha \rangle^{400} - \langle \Delta \alpha \rangle^{200}]$. Without changing the mass-independent constants in the force field, calculations were carried out with arbitrarily assigned masses of 1 to 30 amu for the end atoms. In Fig. 1 we show the results of these studies. At the same time we examined the mass dependence of $r\langle \Delta \alpha \rangle$ and $\langle \Delta r \rangle$ at 300 K for these molecules. These are of importance in determining NMR isotope shifts. In Fig. 1, the values for the dynamic averages using the actual masses of the atoms in the molecule are shown with filled symbols, the other values for arbitrary masses with open symbols.

First let us summarize the mass dependence of $\langle \Delta r \rangle$ and $\langle \Delta \alpha \rangle$ at 300 K in Fig. 1: (a) The behavior of $\langle \Delta r \rangle^{300}$ is as expected, decreasing with increasing mass of the end atom. The vibrational part of this change is easily estimated, as shown in a previous paper.⁹ (b) The isotope effect on $\langle \Delta \alpha \rangle$ upon substitution of the end atoms has different signs, a result of the different mass dependence of the rotational and vibrational contributions. The change with mass of $\langle \Delta \alpha \rangle_{\text{vib}}$ is of either sign but always such as to bring the mean bond angle closer to the equilibrium value as the masses of the end

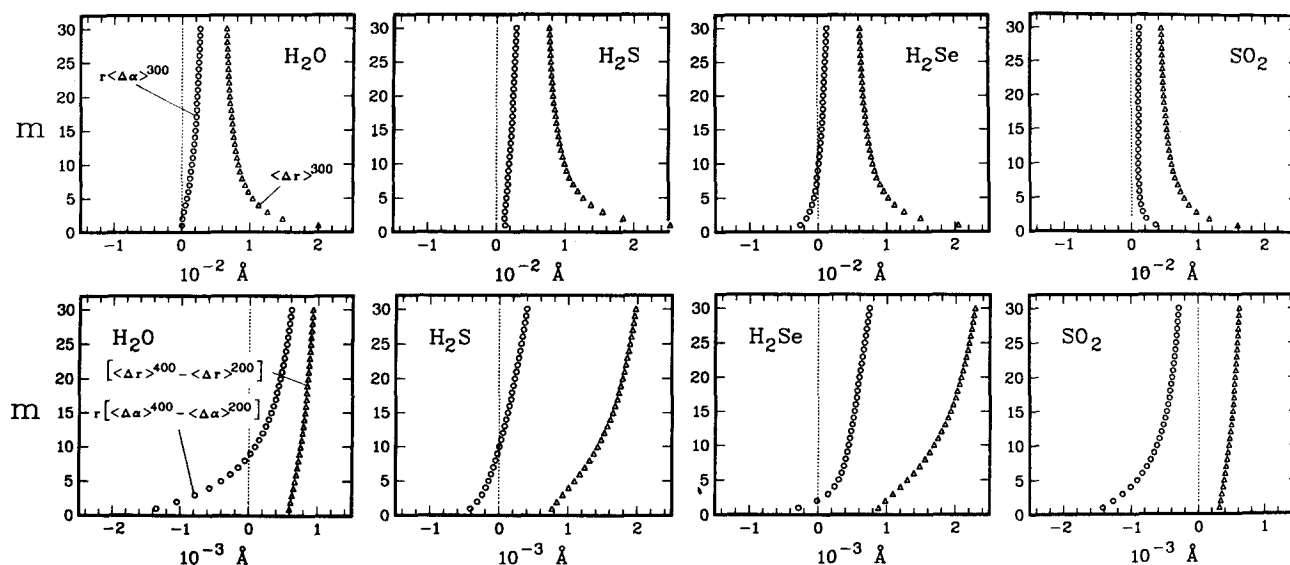


FIG. 1. The mass dependence of $\langle \Delta r \rangle^{300}$, $r\langle \Delta \alpha \rangle^{300}$, $[\langle \Delta r \rangle^{400} - \langle \Delta r \rangle^{200}]$, and $r[\langle \Delta \alpha \rangle^{400} - \langle \Delta \alpha \rangle^{200}]$ in the bent triatomic molecules. The mass of the end atoms are varied arbitrarily keeping the same force field.

atoms increase. On the other hand, the change with mass of $\langle \Delta \alpha \rangle_{\text{rot}}$ is always the same sign, the bond angle increases with increasing mass. (c) The mass dependence of $\langle \Delta r \rangle$ is greater than that of $r\langle \Delta \alpha \rangle$ in all cases. For example, $[\langle \Delta r_{\text{XH}} \rangle - \langle \Delta r_{\text{XD}} \rangle] > r[\langle \Delta \alpha_{\text{HXH}} \rangle - \langle \Delta \alpha_{\text{DXD}} \rangle]$ by a factor of 6 to 80.

C. Implications for NMR measurements

The implications of these findings with respect to NMR isotope shifts are as follows: For the hydrides the contribution to the shielding from the change in $\langle \Delta \alpha \rangle$ with mass, whatever its sign, can be neglected compared with the mass effect on $\langle \Delta r \rangle$, so the isotope shifts are expected to be normal, just as in the AX_n -type molecules (e.g., CH_4), where there is no bond angle deformation contribution to the isotope shift. For O_3 , SO_2 , and SeO_2 , the change in $\langle \Delta r \rangle$ upon ^{18}O substitution is also greater than the change in $\langle \Delta \alpha \rangle$, by a factor of 6 to 60. For all these bent triatomic molecules, the isotope shift is expected to be of normal sign, provided that $(\partial\sigma/\partial\Delta r)_e < 0$. All empirical values of $(\partial\sigma/\partial\Delta r)_e$ which have been determined are found to be negative.^{2,4,5,27} Theoretical values of this derivative for a variety of diatomic molecules have been found to be negative, with the sole exception of Li in LiH.²⁹ Therefore, we should expect normal isotope shifts in nearly all cases. Furthermore, because the change in $\langle \Delta r \rangle$ greatly exceeds the change in $\langle \Delta \alpha \rangle$ upon isotopic substitution of the end atoms in a bent triatomic molecule, the mass dependence of the NMR isotope shift will follow the mass dependence of $\langle \Delta r \rangle$ itself. Therefore, it appears that the additional bond angle deformation term does not significantly affect the isotope shift. This explains why we had been able to find a perfect linear relation between the m'/m -Se-induced isotope shifts in the ^{77}Se resonance of R_1SeSeR_2 compounds and $(m' - m)/m'$, a factor in the mass dependence of $\langle \Delta r_{\text{SeSe}} \rangle$ despite the bond angle deformation terms around the Se in this molecule.³⁰ This also means that the reduced isotope shift, as defined previously [Eq. (5)] is meaningful

even for molecular structures involving bond angle deformations, so long as substitution at end atoms is involved.

Now we consider the temperature dependence of the mean bond properties. The temperature dependence of $\langle \Delta r \rangle$ is the same in all cases, $[\langle \Delta r \rangle^{400} - \langle \Delta r \rangle^{200}] > 0$, tending to increase with increasing mass of end atoms. We note in Fig. 1 that all bent triatomic molecules show the same mass dependence of $r[\langle \Delta \alpha \rangle^{400} - \langle \Delta \alpha \rangle^{200}]$, changing sign, negative for light end atoms, becoming positive for heavier end atoms. The centrifugal stretching due to rotation has an important role in this behavior. The apparent dichotomy in the magnitudes and signs of $r[\langle \Delta \alpha \rangle^{400} - \langle \Delta \alpha \rangle^{200}]$ for hydrides vs oxides arises largely from the mass effect. Although all the curves in Fig. 1 show similar behavior, for the actual masses of these molecules, negative values of $r[\langle \Delta \alpha \rangle^{400} - \langle \Delta \alpha \rangle^{200}]$ are appropriate for the light end atoms, and positive or nearly zero values for heavier end atoms. The qualitative features of the temperature-dependent dynamic behavior relating to $r\langle \Delta \alpha \rangle$, shown in Fig. 1, are retained when different force fields are used, because of the dominance of the rotational contribution, which depends only on the harmonic force field. Of particular importance to the rotational contribution are the off-diagonal elements of the F_S matrix for the A_1 modes.

The implications of these findings with respect to the temperature dependence of the nuclear shielding in the gas at the zero-pressure limit are very interesting. If we assume that $(\partial\sigma/\partial\Delta r)_e < 0$ as is usual, then for O_3 , SO_2 , SeO_2 , the ^{17}O , ^{33}S , and ^{77}Se temperature dependences are expected to be in the normal direction. In these molecules the temperature dependence of the shielding will be dominated by $[\langle \Delta r \rangle^{400} - \langle \Delta r \rangle^{200}]$. On the other hand, the temperature dependence of $r\langle \Delta \alpha \rangle$ in the hydrides is dominated by rotation and thus gives a contribution to the temperature dependence of shielding which is opposite in sign to that of the $\langle \Delta r \rangle$ contribution. Here, depending on the relative signs and mag-

nitudes of $(\partial\sigma/\partial\Delta r)_e$ and $(\partial\sigma/\partial\Delta\alpha)_e$, it may be possible to observe an abnormal temperature dependence, the $\langle\Delta\alpha\rangle$ temperature dependence providing a contribution which is opposite in sign to the normal one.

Some interesting trends in the dynamic behavior can be observed in the results shown in Table III with respect to the position of the apex atom in group VI of the periodic table. For the hydrides, both $[\langle\Delta r\rangle^{400} - \langle\Delta r\rangle^{200}]$ and $r[\langle\Delta\alpha\rangle^{400} - \langle\Delta\alpha\rangle^{200}]$ increase algebraically with the apex atom further down the group. Given that the derivatives of nuclear shielding tend to vary periodically with the electronic average $\langle 1/r^3 \rangle$, just as the paramagnetic term in the shielding does, then the temperature dependent chemical shift in the isolated molecules tends to become more pronounced (with normal sign) in going from O to S to Se. This means that the best opportunity to observe an abnormal temperature dependence of $\sigma_0(T)$ is for ^{17}O in H_2O , and the worst for ^{77}Se in H_2Se . Unfortunately, because of the strong hydrogen bonding in H_2O , dimers will be present even at very low densities. The temperature dependence of shielding will be determined by the temperature-dependent monomer-dimer equilibrium and determination of $\sigma_0(T)$ will be extremely difficult if not impossible.

From the reported isotope shift³¹ and the negligible isotope effect on $r\langle\Delta\alpha\rangle$ in H_2Se , we calculate from the $[\langle\Delta r_{\text{SeH}}\rangle - \langle\Delta r_{\text{SeD}}\rangle]$ in Table III an estimate for the derivative $(\partial\sigma^{\text{Se}}/\partial\Delta r_{\text{SeH}})_e \simeq -1250 \text{ ppm/\AA}$. The temperature dependence of the nuclear shielding in the zero-pressure limit would then be $\sigma_0(400) - \sigma_0(200) \simeq -1250 \times 2 \times 0.88 \times 10^{-3} + (\partial\sigma/\partial r\Delta\alpha)_e(-0.28 \times 10^{-3})$. An abnormal temperature dependence will be observed only if $(\partial\sigma/\partial r\Delta\alpha)_e < -7900 \text{ ppm/\AA}$. Therefore, it is quite likely that the temperature dependence of ^{77}Se resonance in the gas phase will be normal.

When the magnitude of $(\partial\sigma/\partial\Delta\alpha)_e$ is small, whatever its sign, a normal temperature dependence will be observed. For example, for ^{17}O in H_2O , with the theoretical derivatives $(\partial\sigma^{\text{O}}/\partial\Delta r)_e = -270.9 \text{ ppm/\AA}$ and $(\partial\sigma^{\text{O}}/\partial\Delta\alpha)_e = -27.3 \text{ ppm/rad}$, Fowler and Raynes predict $(d\sigma^{\text{O}}/dT) = -1.52 \times 10^{-3} \text{ ppm/deg}$.¹⁸ Calculations by Schindler and Kutzelnigg on H_2O yield similar results.³² They also find deshielding of ^{17}O with increase in bond angle and with increase in O-H bond length: $(\partial\sigma^{\text{O}}/\partial\Delta r)_e \simeq -285 \text{ ppm/\AA}$ and $(\partial\sigma^{\text{O}}/\partial\Delta\alpha)_e \simeq -7 \text{ ppm/rad}$. Using these values we predict $(d\sigma^{\text{O}}/dT) = -1.64 \times 10^{-3} \text{ ppm/deg}$. On the other hand, we can calculate $(\partial\sigma^{\text{O}}/\partial\Delta r)_e$ from the observed isotope shift and our $\langle\Delta r\rangle$ values in Table III, neglecting the contribution to the isotope shift by the terms in $\langle\Delta\alpha\rangle$. We obtain $(\partial\sigma^{\text{O}}/\partial\Delta r)_e = -294 \text{ ppm \AA}^{-1}$, which compares very well with the *ab initio* theoretical values -270.9 and $-285 \text{ ppm \AA}^{-1}$.

The spin-rotation constants for ^1H and ^2D in the molecules H_2S , HDS , and D_2S have recently been measured by molecular beam electric resonance.³³ These would provide measures of the isotope shifts $^2\Delta ^1\text{H}(^{2/1}\text{H})$ or $^2\Delta ^2\text{H}(^{2/1}\text{H})$. However, it was found that there is no statistically significant difference in the tensors calculated from H or D in the three isotopomers, indicating that these NMR isotope shifts will be small.

For ^{17}O in O_3 , theoretical calculations of shielding for various bond lengths and bond angles¹⁹ allow us to deduce the shielding derivatives: $(\partial\sigma^{\text{end}}/\partial\Delta r)_e = -2.0 \times 10^4$, $(\partial\sigma^{\text{apex}}/\partial\Delta r)_e = -1.9 \times 10^4 \text{ ppm/\AA}$, and $(\partial\sigma^{\text{end}}/\partial\Delta\alpha)_e = -600$, $(\partial\sigma^{\text{apex}}/\partial\Delta\alpha)_e = -1250 \text{ ppm/rad}$ at $r = 1.2 \text{ \AA}$ (not the equilibrium r_e). Unfortunately the authors varied the bond angle for a fixed bond length other than equilibrium one. These derivatives appear to be unusually large even for a molecule that exhibits Van Vleck paramagnetism. Nevertheless, we use these derivatives with our $\langle\Delta r\rangle^T$ and $\langle\Delta\alpha\rangle^T$ values from Table III to calculate the expected temperature dependence for ^{17}O shielding in this molecule: $[\sigma_0(T) - \sigma_0(300)] = -0.8 \times 10^{-1}(T - 300) \text{ ppm}$ for the end ^{17}O and $-1.5 \times 10^{-1}(T - 300) \text{ ppm}$ for the apex ^{17}O . We also calculate the $^{18/16}\text{O}$ -induced isotope shift for the apex ^{17}O : $\sigma(^{17}\text{O}^{16}\text{O}_2) - \sigma(^{17}\text{O}^{18}\text{O}_2) = -8.6 \text{ ppm}$. These are very large shifts but they are in the normal direction. It would be interesting to observe the shielding in this molecule in the gas phase as a function of temperature. Only the condensed phase data are available, and these cannot be compared directly with the theoretical shielding for the end and apex ^{17}O .³⁴ The necessary gas-to-liquid shift corrections of the condensed phase data are expected to be large for this system.

IV. TRIGONAL PYRAMIDAL CASE

Although the anharmonic force fields are not as well established for these molecular types as they are for the bent triatomics, some dynamic calculations are necessary to explain the observed abnormal behavior of $\sigma_0(T)$ for N and P in NH_3 and PH_3 ,^{10,11} in contrast with normal behavior for P in PF_3 .¹² For this purpose, we use the best available harmonic force fields and augment these with Morse anharmonic stretching and cubic force constants from model potential functions for nonbonded atoms, using the method described earlier.⁵

We still neglect the bending anharmonicity. A source of H_3 , the cubic Urey-Bradley force constant for angle deformation in NH_3 is the model potential for the inversion which is used to fit the microwave spectrum. The energy splittings resulting from the double-well potential can be reproduced fairly well by several model functions.³⁵ However, the potential functional forms do not necessarily give the appropriate shape (anharmonicity) at the bottom of the wells. H_3 is the cubic bending force constant appropriate to a pyramidal equilibrium geometry, whereas the inversion splittings are not so sensitive to the shape of the model potential as to the height of the barrier in it, far removed from the equilibrium pyramidal geometry. Nevertheless, the third derivatives of these model potentials with respect to the angle can be related to F_3 and H_3 , the nonbonded and the bending cubic force constants, respectively, the Bartell's modified anharmonic force field. We obtain values of H_3 which are positive, as Bartell does.²⁶ However, the magnitudes vary from one model function to another, so that we are unable to obtain a unique value of H_3 for ammonia. The inversion potential for the other molecules PH_3 , NF_3 , and PF_3 are less well known. Therefore, we neglect H_3 altogether.

TABLE IV. Potential parameters used in dynamical calculations for pyramidal molecules.

	NH ₃ ^{a, b}	PH ₃ ^c	NF ₃ ^d	PF ₃ ^{e, f}
$r_e/\text{\AA}$	1.0116	1.4116	1.3650	1.5610
α/deg	107.2	93.33	102.4	97.7
$F_{11}/\text{mdyn \AA}^{-1}$	7.0815	3.3410	5.765	6.4150
F_{12}	0.7195	0.0708	0.57	0.4369
F_{22}	0.5196	0.3071	1.368	0.8146
F_{33}	7.0371	3.3390	3.364	5.0210
F_{34}	-0.1743	-0.0340	-0.316	-0.1742
F_{44}	0.6649	0.3663	0.901	0.5068
$F_3^g/\text{mdyn \AA}^{-1}$	-2.2586	-0.7113	-10.558	-2.524
$a_m^h/\text{\AA}^{-1}$	2.283	1.514	1.939	1.807

^a Reference 35.^b Reference 36.^c J. L. Duncan and D. C. McKean, J. Mol. Spectrosc. **107**, 301 (1984).^d A. Allan, J. L. Duncan, J. H. Holloway, and D. C. McKean, J. Mol. Spectrosc. **31**, 368 (1969).^e Y. Kawashima and A. P. Cox, J. Mol. Spectrosc. **65**, 319 (1977).^f C. E. Small and J. G. Smith, J. Mol. Spectrosc. **73**, 215 (1978).^g Calculated using the nonbonded potential from R. H. Boyd and L. Kesner, J. Chem. Phys. **72**, 2179 (1980), for H-H interactions and a Lennard-Jones potential from J. Kestin, S. T. Rao, and W. Wakeham, Physica **58**, 165 (1972) for the F-F interactions.^h Calculated using Herschbach and Laurie's exponential function [D. R. Herschbach and V. W. Laurie, J. Chem. Phys. **35**, 450 (1961)] and the actual bond lengths.

A. Dynamic calculations

The method of calculation of mean bond displacements in the pyramidal molecule is analogous to that for the bent triatomic molecule, except that the force constants appearing in equations analogous to Eqs. (7) and (8) include F_3 and the Morse parameter a . The parameters used for the NH₃, PH₃, NF₃, and PF₃ molecules are given in Table IV. The results are shown in Table V.

The rotational contribution to the temperature dependence of $\langle \Delta r \rangle$ agrees with the results of Toyama *et al.*²⁸ who obtained $\langle \Delta r_{\text{NH}} \rangle_{\text{rot}} = 2.24 \times 10^{-6} \text{T}$ and $r\langle \Delta \alpha \rangle_{\text{rot}} = -3.15 \times 10^{-6} \text{T \AA}$ for NH₃, $\langle \Delta r_{\text{ND}} \rangle_{\text{rot}} = 2.11 \times 10^{-6} \text{T}$ and $r\langle \Delta \alpha \rangle_{\text{rot}} = -1.76 \times 10^{-6} \text{T \AA}$ for ND₃. These may be compared to our values: $2.26 \times 10^{-6} \text{T}$, $-3.31 \times 10^{-6} \text{T}$, $2.13 \times 10^{-6} \text{T}$, and $-1.98 \times 10^{-6} \text{T \AA}$, respectively. The vibrational contribution to $\langle \Delta r \rangle$ and $r\langle \Delta \alpha \rangle$ have been calculated by Bartell²⁶: $\langle \Delta r \rangle_{\text{vib}} = 0.0237$ and 0.0174\AA for NH₃ and ND₃, respectively, and $r\langle \Delta \alpha \rangle_{\text{vib}} = 0.0223$ and 0.0162

\AA , respectively for NH₃ and ND₃. Morino *et al.*³⁶ report $\langle \Delta r \rangle_{\text{vib}} = 0.0208$ and 0.0161\AA and $r\langle \Delta \alpha \rangle_{\text{vib}} = 0.0115$ and 0.0092\AA for NH₃ and ND₃. Our corresponding values are 0.202 and 0.0146\AA for $\langle \Delta r \rangle_{\text{vib}}$ and -0.007 and -0.004\AA for $r\langle \Delta \alpha \rangle_{\text{vib}}$. All values are at 0 K. While the mean bond displacements are in good agreement, the mean bond angle deformations are not of the same sign.

The sign of $\langle \Delta \alpha \rangle_{\text{vib}}$ obtained by Bartell differs from ours because he neglected the off-diagonal elements in the mean square amplitudes in solving the coupled equations in $\langle \Delta r \rangle$ and $\langle \Delta \alpha \rangle$. Some of these are opposite in sign to the diagonal elements which he did include. Morino *et al.*³⁶ on the other hand, neglected the cubic force constants $f_{\alpha\alpha\alpha}$ and $f_{\alpha\alpha'\alpha'}$ which give rise to cross terms in $\langle \Delta \alpha \rangle$ which are opposite in sign to the terms in $f_{\alpha\alpha\alpha}$. Most of $\langle \Delta \alpha \rangle_{\text{vib}}$ contributions are due to terms in $f_{\alpha\alpha\alpha}$ and $f_{\alpha\alpha'\alpha'}$. These were assumed to be equal whereas in other systems, where these cubic force constants are known, they are sometimes of opposite sign. Their cubic force constants in the dimensionless normal co-

TABLE V. Mean bond displacements, mean bond angle deformation isotope effects, and temperature dependence for selected pyramidal molecules (see Table III for definitions of symbols).

	$\langle \Delta r \rangle$			$r\langle \Delta \alpha \rangle$		
	Vib.	Rot.	Tot.	Vib.	Rot.	Tot.
NH ₃ /10 ⁻² \AA	2.018	0.068	2.086	-0.675	-0.099	-0.775
ND ₃ /10 ⁻² \AA	1.466	0.064	1.529	-0.429	-0.059	-0.488
$\Delta_{\text{iso}}/10^{-3} \text{\AA}$	5.522	0.041	5.563	-2.462	-0.401	-2.864
$\Delta_T/10^{-4} \text{\AA}$	0.510	4.526	5.030	0.915	-6.628	-5.713
PH ₃ /10 ⁻² \AA	1.972	0.088	2.060	1.262	-0.010	1.252
PD ₃ /10 ⁻² \AA	1.423	0.087	1.510	0.957	0.011	0.967
$\Delta_{\text{iso}}/10^{-3} \text{\AA}$	5.589	0.004	5.494	3.155	-0.211	2.879
$\Delta_T/10^{-4} \text{\AA}$	1.300	5.867	7.160	3.990	0.702	3.290
NF ₃ /10 ⁻² \AA	0.673	0.048	0.722	0.574	0.041	0.615
$\Delta_T/10^{-4} \text{\AA}$	9.691	3.237	12.928	13.702	2.737	16.439
PF ₃ /10 ⁻² \AA	0.455	0.038	0.493	0.230	0.050	0.280
$\Delta_T/10^{-4} \text{\AA}$	6.460	2.530	8.990	8.925	3.326	12.252

ordinates k_{244} and k_{134} are opposite in sign to those obtained using a nonbonded interactions (van der Waals) model. However, this disagreement in the sign of $\langle\Delta\alpha\rangle_{\text{vib}}$ in NH_3 is largely irrelevant to our conclusions here, because the rotational contribution dominates the magnitude and temperature dependence of $\langle\Delta\alpha\rangle$.

An additional complication may arise from the inversion motion in NH_3 in the evaluation of the contributions to the mean bond displacements. The constants which appear in the formulas for rotational contribution arise from the derivatives of the moments of inertia with respect to normal coordinates for a molecule with an equilibrium configuration of a rigid C_{3v} symmetric top. With inversion, these become functions of the inversion parameter. The same considerations apply to the vibrational contribution. The force constants are quadratic and cubic derivatives of the potential energy for molecule with an equilibrium pyramidal configuration. With inversion these force constants become functions of the inversion parameter. However, the lowest inversion barrier among the molecules studied here is that in NH_3 , for which it is $2076\text{ cm}^{-1} > kT$ at room temperature. Thus, around room temperature, vibrational averaging occurs mostly around that part of the potential which is well below the barrier in NH_3 , certainly also in PH_3 , NF_3 , and PF_3 .

Our $\langle\Delta\alpha\rangle_{\text{rot}}$ results for PH_3 appear to be of doubtful validity. The rotational contribution to the mean bond angle deformation depends on the off-diagonal elements of the F

matrix for totally symmetric vibrations. In PH_3 these are very small compared to NH_3 , NF_3 , and PF_3 : While F_{12}/F_{11} is about 10% in these molecules, the ratio is only about 2% in PH_3 . In plots of the type shown in Fig. 1, PH_3 does not behave like H_2S with respect to the mass and temperature dependence of $\langle\Delta\alpha\rangle_{\text{rot}}$, whereas NH_3 has the same behavior as H_2O . The vibrational contribution to $\langle\Delta\alpha\rangle$ appears to be unusually large. Earlier harmonic force fields for PH_3 do not yield results which are any more consistent than these. Therefore, we ignore our results for $\langle\Delta\alpha\rangle$ for PH_3 altogether.

B. Comparison with bent triatomics

In a comparative study, we find analogous qualitative behavior in the mass and temperature dependence of the mean bond displacements and mean bond angle deformations in the pyramidal molecules compared to the bent triatomics. These results are shown in Fig. 2. The PF_3 curves are very similar to those for NF_3 . The similarities which are observed between the pyramidal and bent triatomic molecules are the following:

- (1) The magnitude of $\langle\Delta r\rangle$ is dominated by the vibrational contribution in all cases.
- (2) The mass effect on $\langle\Delta r\rangle$ is dominated by vibration in all cases, $\langle\Delta r\rangle$ always decreases with increasing mass of the end atoms.
- (3) The mass dependence of $r\langle\Delta\alpha\rangle$ is small compared to the mass dependence of $\langle\Delta r\rangle$.

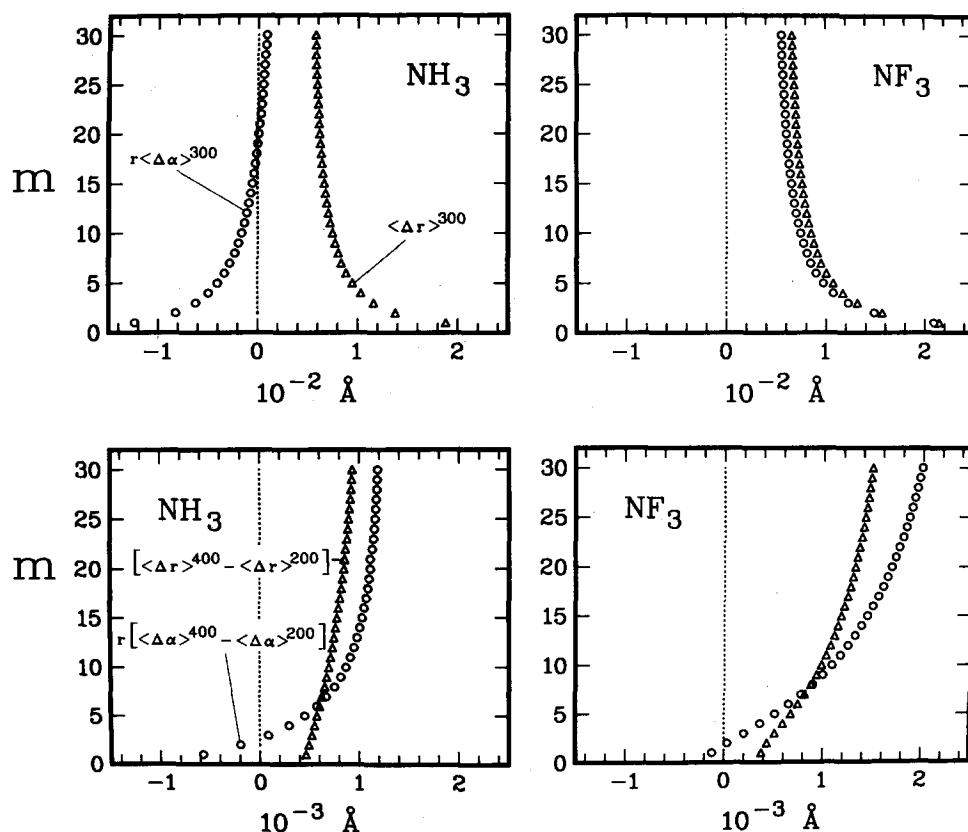


FIG. 2. The mass dependence of $\langle\Delta r\rangle^{300}$, $r\langle\Delta\alpha\rangle^{300}$, $[\langle\Delta r\rangle^{400} - \langle\Delta r\rangle^{200}]$, and $r[\langle\Delta\alpha\rangle^{400} - \langle\Delta\alpha\rangle^{200}]$ in the pyramidal molecules. The mass of the end atoms are varied arbitrarily, keeping the same force field.

(4) The temperature dependence of $\langle\Delta r\rangle$ is dominated by the rotational contribution for the hydrides. For the oxides and fluorides the rotational and vibrational contributions to $\langle\Delta r\rangle$ are of comparable magnitudes.

(5) For the bent oxides and pyramidal fluorides the temperature dependence of $\langle\Delta r\rangle$ dominates over that of $\langle\Delta\alpha\rangle$ in cases where they are opposite in direction, or else they are the same sign and give an enhanced effect.

(6) The temperature dependence of $\langle\Delta\alpha\rangle_{\text{vib}}$ is small for hydrides and large for oxides (or fluorides).

(7) The temperature dependence of $\langle\Delta\alpha\rangle$ in NH_3 is the same direction as that of the bent hydrides and is dominated by rotation.

(8) The mass dependence of $[\langle\Delta r\rangle^{400} - \langle\Delta r\rangle^{200}]$ in NH_3 parallels that of H_2O , H_2S , and H_2Se while the fluorides parallel those of the oxides.

These similarities in behavior between NH_3 and the bent hydrides on one hand, and the pyramidal fluorides and the bent oxides on the other, call attention to the inconsistency of the PH_3 $\langle\Delta\alpha\rangle$ results with the rest of the molecular systems studied here. Therefore, we hesitate to draw any conclusions based on the calculated $\langle\Delta\alpha\rangle$ in PH_3 .

C. Implications for NMR measurements

The implications of these findings with respect to the temperature dependence of the nuclear shielding in the zero-pressure limit are as follows: Semiempirical theoretical calculations of N and P shielding in NH_3 , NF_3 , PH_3 , and PF_3 indicate that $(\partial\sigma/\partial\Delta r)_e < 0$ for all nuclei in these molecules.³⁷ This is consistent with all known empirical and theoretical values of $(\partial\sigma/\partial\Delta r)_e$. The semiempirical calculations also indicate that $(\partial\sigma/\partial\Delta\alpha)_e < 0$ for N in NH_3 and NF_3 and for P in PH_3 , but $(\partial\sigma/\partial\Delta\alpha)_e > 0$ for P in PF_3 . The latter is opposite to earlier results of Van Wazer which indicated $(\partial\sigma/\partial\Delta\alpha)_e < 0$ for P in PF_3 .³⁸ If we take both $(\partial\sigma/\partial\Delta r)_e$ and $(\partial\sigma/\partial\Delta\alpha)_e$ to be negative for the apex nucleus in pyramidal molecules, then the temperature dependence of NH_3 can be abnormal, provided the $r[\langle\Delta\alpha\rangle^{400} - \langle\Delta\alpha\rangle^{200}]$ term overcomes the oppositely signed $[\langle\Delta r\rangle^{400} - \langle\Delta r\rangle^{200}]$ term. On the other hand, both terms have the same sign in NF_3 and PF_3 so $\sigma_0(T)$ should be normal for the N and P nuclei in these molecules. Thus, we have an explanation for the abnormal temperature dependence of σ_0 for ^{15}N in NH_3 and normal σ_0 for P in PF_3 . We also predict that the ^{15}N in NF_3 behavior at the zero-pressure limit will be normal. Due to the inconsistency of the $\langle\Delta\alpha\rangle$ results for PH_3 relative to the general behavior of the molecular systems studied here, we cannot draw any valid *a priori* explanations for the abnormal behavior of $\sigma_0(T)$ for ^{31}P in PH_3 .

The smaller mass effect on $\langle\Delta\alpha\rangle$ compared to the mass effect on $\langle\Delta r\rangle$ is consistent with normal isotope shifts for all apex nuclei considered here, with an isotopic mass dependence which largely reflects that of $\langle\Delta r\rangle$ for substitution at the end atoms. This mass dependence of the isotope shift has been previously studied in molecules involving no mean bond angle deformation.³⁰ Those results will be largely valid also for the molecular types considered here.

Using the measured temperature dependence of ^{15}N shielding in the zero-pressure limit in NH_3 gas $(d\sigma_0/dT$

$= +0.0065 \pm 0.0008 \text{ ppm/deg})^{10}$ and the observed ^2D -induced ^{15}N isotope shift (-0.65 ppm per D),³⁹ we obtain estimates of both derivatives: $(\partial\sigma_0/\partial\Delta r)_e \simeq -2350 \text{ ppm/\AA}$ and $(\partial\sigma_0/\partial\Delta\alpha)_e \simeq -4400 \text{ ppm/rad}$. These estimates for the derivatives are very sensitive to the force field used for NH_3 because both the isotope shift and the temperature dependence of $\sigma_0(T)$ result from $\langle\Delta r\rangle$ and $\langle\Delta\alpha\rangle$ terms of opposite signs. A good shielding surface and a good potential energy surface for NH_3 are both required for a quantitative interpretation of the experimental data. We have shown only that the mass and temperature dependence of $\langle\Delta r\rangle$ and $\langle\Delta\alpha\rangle$ are opposite, which makes it possible to obtain a normal isotope shift and an abnormal temperature dependence for ^{15}N in NH_3 . If the mean bond angle deformation of PH_3 had a mass and temperature dependence similar to that in NH_3 , then the explanation for the unusual sign of $(d\sigma_0/dT)$ reported for ^{31}P in PH_3 would be the same as in NH_3 .

V. ELECTRON REDISTRIBUTION WITH NUCLEAR MOTION

Theoretical calculations and photoelectron spectroscopy data show that the highest occupied molecular orbital in each of the molecules considered here (OH_2 , SH_2 , SeH_2 , O_3 , SO_2 , SeO_2 , NH_3 , PH_3 , NF_3 , PF_3) consists primarily of a lone-pair *s-p* hybrid on the central atom.⁴⁰ The lowest excitation energy corresponds to the magnetic dipole allowed $a_1(\text{lone pair}) \rightarrow e$ excitation in the pyramidal molecules and the corresponding $b_1(\text{lone pair}) \rightarrow a_1$ excitation in the bent triatomics. Thus, the lone pair on the central atom has an important role in paramagnetic shielding of its nucleus. The method of calculation using different gauge origins for different localized molecular orbitals (IGLO)³² which permits assignment of the shielding contributions to individual localized molecular orbitals has shown that this is the case for OH_2 and NH_3 . In O_3 especially, it has been found that the paramagnetic contributions come mainly from the lone pairs of the respective oxygen atoms and not from the sigma bonds. The contribution of the lone pair to the change in shielding with bond extension or bond angle deformation is therefore of special interest here. In particular, it would be useful to have a model for the change in shielding as the bond geometry changes, in order to be able to explain why the isotope shifts are larger for central nuclei with lone pairs. For this purpose, we examine the behavior of the electron distributions as nuclei vibrate away from their equilibrium positions.

We have previously noted that deshielding of the nuclei occurs with the relaxation in the molecular charge distribution upon displacement of the nuclei in diatomic molecules.⁴¹ These effects are illustrated in the form of shielding density difference maps between the extended and the equilibrium internuclear separation. These are consistent with the observations based on charge density difference maps⁴²: Charge density is removed from both sides of the displaced nucleus (of an electronegative atom such as N, O, F) and concentrated in a region perpendicular to the bond axis at the position of the nucleus. This quadrupolar polarization leads to a deshielding of the displaced nucleus, as is indeed shown by the shielding density difference maps for HF, leading to $(\partial\sigma/\partial\Delta r)_e < 0$. A similar examination of the changes in the

electron distributions as the bond angle changes should provide an interpretation of $(\partial\sigma/\partial\Delta\alpha)_e$.

An *ab initio* study in H_2O , H_2S , and NH_3 , in which all the bond lengths were held fixed at their equilibrium values and all bond angles were allowed to vary, has demonstrated the changes in the bond pair and lone pair electron distributions with bond angle deformation.⁴³ The surprising result is that as the nuclei vibrate away from their equilibrium positions, the central atom orbitals lag far behind. The implications of these findings on $(\partial\sigma/\partial\Delta\alpha)_e$ are as follows. It has been shown that the contributions from the orbitals centered on the observed nucleus largely determine the paramagnetic shielding. The contributions due to the orbitals centered on H, which completely follow the H nuclei as they move in vibration, are much smaller. In the limit of complete orbital stasis, $(\partial\sigma/\partial\Delta\alpha)_e \simeq 0$ for the central atom shielding. The lack of orbital following in H_2O is consistent with the small magnitude of $(\partial\sigma^\text{O}/\partial\Delta\alpha)_e$ found by Fowler and Raynes,¹⁸ and by Schindler and Kutzelnigg.¹⁹ The oxygen lone pair *p* character does increase with increasing bond angle in H_2O . To a first approximation, this leads to deshielding at the oxygen.⁴⁴ This is consistent with the negative sign of $(\partial\sigma^\text{O}/\partial\Delta\alpha)_e$. For H_2S , the *p* character of the lone pair on sulfur also increases with increasing bond angle. To a first approximation this again gives a deshielding contribution at the sulfur nucleus, leading to $(\partial\sigma^\text{S}/\partial\Delta\alpha)_e < 0$, just as in H_2O . Unfortunately, there are no shielding surface calculations for H_2S with which this may be compared. Results for NH_3 are similar, but the bonding orbital movement accompanying the inversion vibrational mode of NH_3 is unique. As the geometry gets very close to planar, the N bonding orbitals rapidly change direction so that they point straight toward the protons when the nuclei are planar. This is of course accompanied by drastic changes in hybridization. This does not occur until the geometry is very close to planar. At intermediate geometries there is lack of orbital following just as in H_2O and H_2S . In addition, there is an unusual behavior of the bonding and lone pair orbitals in NH_3 : An increase in the H_aNH_b angle is accompanied by partial bonding between the lone pair and each of the hydrogens, especially H_c . This implies that the N shielding has a greater dependence on bond angle than O in H_2O or S in H_2S .

VI. CONCLUSIONS

We have found that the generally larger isotope shifts observed for N in NH_3 compared to NH_4^+ , in NO_2^- compared to NO_3^- , and in general for apex nuclei in molecular structures with nonvanishing mean bond angle deformations, are not due to a sizeable contribution from the bond angle deformation but rather to the larger derivatives of nuclear shielding with respect to bond extension. These larger derivatives can be attributed to the generally greater paramagnetic shielding term in these molecules, partly due to the role played by the lone pair electrons on the apex nucleus.

The dynamic behavior of bonds to the end atoms (the temperature and mass dependence of $\langle\Delta r\rangle$) is found to be the same as in molecular structures in which bond angle deformation

is unimportant. The dynamic behavior of $\langle\Delta\alpha\rangle$ (shown in Figs. 1 and 2) shows the same qualitative features for all the hydrides studied here. Likewise, the qualitative features of the curves for the oxides and fluorides are the same for the bent triatomics and the pyramidal molecules. These figures provide the basis for isotope shifts of the usual sign in all these molecules and the unusual temperature dependence of $\sigma_0(T)$ for N in NH_3 . The general conditions under which an abnormal temperature dependence of $\sigma_0(T)$ may arise have been determined. If the mean bond angle deformation of PH_3 behaved just like that in NH_3 , then this would also explain the unusual temperature dependence of $\sigma_0(T)$ observed for ^{31}P in PH_3 . With the dynamic factors in Table V, it is not possible to interpret both the unusual temperature dependence and the usual isotope shift for P in PH_3 using only first derivatives of shielding.

Deshielding of the apex nucleus with an increase in bond angle as is found for ^{17}O in H_2O is consistent with the charge distribution changes which accompany the change in geometry revealed by contour maps derived from *ab initio* calculations of electron densities in the H_2O , H_2S , and NH_3 molecules.

We have given rough empirical estimates of the derivatives $(\partial\sigma/\partial\Delta r)_e$ and $(\partial\sigma/\partial\Delta\alpha)_e$ for ^{15}N in NH_3 . The NH_3 and NH_4^+ molecules with only ten electrons are excellent candidates for large basis set calculations of the shielding surfaces for ^{15}N and ^1H nuclei. Such *ab initio* calculations as are adequate to yield good nuclear shielding surfaces also provide, as a side product, good energy surfaces. The derivatives which characterize these energy surfaces provide *ab initio* force constants for the dynamical averaging such as we have carried out here. Such calculations are predicted to yield larger magnitudes of paramagnetic shielding for ^{15}N in NH_3 than for NH_4^+ , as well as larger magnitudes of $(\partial\sigma^\text{N}/\partial\Delta r)_e$ for NH_3 than for NH_4^+ .

ACKNOWLEDGMENT

This research was supported in part by the National Science Foundation (Grant CHE81-16193).

¹H. Batiz-Hernandez and R. A. Bernheim, *Progr. NMR Spectrosc.* **3**, 63 (1967); P. E. Hansen, in *Annual Reports on NMR Spectroscopy*, edited by G. A. Webb (Academic, New York, 1983), Vol. 15, p. 105.

²R. Ditchfield, *Chem. Phys.* **63**, 185 (1981); C. J. Jameson, *Bull. Magn. Reson.* **3**, 3 (1981).

³P. W. Fowler, G. Riley, and W. T. Raynes, *Mol. Phys.* **42**, 1463 (1981).

⁴C. J. Jameson, *J. Chem. Phys.* **67**, 2814 (1977).

⁵C. J. Jameson and H. J. Osten, *J. Chem. Phys.* **81**, 4915 (1984).

⁶H. J. Osten and C. J. Jameson, *J. Chem. Phys.* **81**, 4288 (1984).

⁷W. Gombler, *J. Am. Chem. Soc.* **104**, 6616 (1982).

⁸W. Gombler, *J. Magn. Reson.* **53**, 69 (1983).

⁹C. J. Jameson and H. J. Osten, *J. Chem. Phys.* **81**, 4300 (1984).

¹⁰C. J. Jameson, A. K. Jameson, S. M. Cohen, H. Parker, D. Oppusunggu, P. M. Burrell, and S. Wille, *J. Chem. Phys.* **74**, 1608 (1981).

¹¹C. J. Jameson, A. K. Jameson, and H. Parker, *J. Chem. Phys.* **68**, 2868 (1978).

¹²C. J. Jameson, A. K. Jameson, and S. Wille, *J. Phys. Chem.* **83**, 3372 (1979).

¹³Y. Morino, *Pure Appl. Chem.* **18**, 323 (1969).

¹⁴B. J. Krohn, W. C. Ermler, and C. W. Kern, *J. Chem. Phys.* **60**, 22 (1974).

¹⁵B. J. Rosenberg, W. C. Ermler, and I. Shavitt, *J. Chem. Phys.* **65**, 4072 (1976); R. J. Bartlett, I. Shavitt, and G. D. Purvis, *ibid.* **71**, 281 (1979).

- ¹⁶A. R. Hoy, I. M. Mills, and G. Strey, *Mol. Phys.* **24**, 1265 (1972).
¹⁷M. Lacy and D. H. Whiffen, *Mol. Phys.* **43**, 47 (1981).
¹⁸P. W. Fowler and W. T. Raynes, *Mol. Phys.* **43**, 65 (1981).
¹⁹M. Schindler and W. Kutzelnigg, *Mol. Phys.* **48**, 781 (1983).
²⁰A. I. Skotnikov and L. M. Sverdlov, *Opt. Spectrosc.* **42**, 49 (1977).
²¹R. J. Mawhorter and M. Fink, *J. Chem. Phys.* **79**, 3292 (1983).
²²B. Kohl and D. L. Hilderbrandt, *J. Mol. Struct. Theochem.* **85**, 25, 325 (1981).
²³R. J. Whitehead and N. C. Handy, *J. Mol. Spectrosc.* **55**, 356 (1975), **59**, 459 (1976).
²⁴K. Kuchitsu and Y. Morino, *Bull. Chem. Soc. Jpn.* **38**, 814 (1965).
²⁵S. Carter, I. M. Mills, J. N. Murrell, and A. J. C. Varandas, *Mol. Phys.* **45**, 1053 (1982).
²⁶L. S. Bartell, *J. Chem. Phys.* **38**, 1827 (1963).
²⁷C. J. Jameson and H. J. Osten, *J. Chem. Phys.* **81**, 2556 (1984).
²⁸M. Toyama, T. Oka, and Y. Morino, *J. Mol. Spectrosc.* **13**, 193 (1964).
²⁹R. M. Stevens and W. N. Lipscomb, *J. Chem. Phys.* **40**, 2238 (1964).
³⁰C. J. Jameson and H. J. Osten, *J. Chem. Phys.* **81**, 4293 (1984).
³¹H. J. Jakobsen, A. J. Zozulin, P. D. Ellis, and J. D. Odom, *J. Magn. Reson.* **38**, 219 (1980).
³²M. Schindler and W. Kutzelnigg, *J. Chem. Phys.* **76**, 1919 (1982).
³³R. Viswanathan and T. R. Dyke, *J. Mol. Spectrosc.* **103**, 231 (1984).
³⁴A. E. Florin and M. Alei, *J. Chem. Phys.* **47**, 4268 (1967).
³⁵V. Spirko, J. M. R. Stone, and D. Papousek, *J. Mol. Spectrosc.* **60**, 159 (1976).
³⁶Y. Morino, K. Kuchitsu, and S. Yamamoto, *Spectrochim. Acta Part A* **24**, 335 (1968).
³⁷B. T. Hamdi, D. J. Reynolds, and G. A. Webb, *Org. Magn. Reson.* **22**, 90 (1984).
³⁸J. H. Letcher and J. R. Van Wazer, *J. Chem. Phys.* **44**, 815 (1966).
³⁹W. M. Litchman, M. Alei, and A. E. Florin, *J. Chem. Phys.* **50**, 1897 (1969).
⁴⁰J. P. Maier and D. W. Turner, *J. Chem. Soc. Faraday Trans. 2*, **1972**, 711; S. X. Xiao, W. C. Trogler, D. E. Ellis, and Z. B. Yellin, *J. Am. Chem. Soc.* **105**, 7034 (1983).
⁴¹C. J. Jameson and A. D. Buckingham, *J. Chem. Phys.* **73**, 5684 (1980).
⁴²R. F. W. Bader and A. D. Bandrauk, *J. Chem. Phys.* **49**, 1666 (1968).
⁴³D. M. Chipman, W. E. Palke, and B. Kirtman, *J. Am. Chem. Soc.* **102**, 3377 (1980).
⁴⁴M. Karplus and T. P. Das, *J. Chem. Phys.* **34**, 1683 (1961).